Proc. Natl. Acad. Sci. USA
Vol. 94, pp. 14770–14775, December 1997
Neurobiology

N-methyl-D-aspartate receptor activation and visual activity induce elongation factor-2 phosphorylation in amphibian tecta: A role for *N*-methyl-D-aspartate receptors in controlling protein synthesis

A. J. SCHEETZ*†, ANGUS C. NAIRN‡, AND MARTHA CONSTANTINE-PATON*

*Yale University, Department of Biology, Kline Biology Tower, P.O. Box 208103, New Haven, CT 06520-8103; and ‡Rockefeller University, Laboratory of Molecular and Cellular Neuroscience, Box 296, 1230 York Avenue, New York, NY 10021

Edited by William T. Greenough, University of Illinois, Urbana, IL, and approved October 23, 1997 (received for review July 9, 1997)

ABSTRACT ***N*-methyl-D-aspartate receptor (NMDAR) activation has been implicated in forms of synaptic plasticity involving long-term changes in neuronal structure, function, or protein expression. Transcriptional alterations have been correlated with NMDAR-mediated synaptic plasticity, but the problem of rapidly targeting new proteins to particular synapses is unsolved. One potential solution is synapse-specific protein translation, which is suggested by dendritic localization of numerous transcripts and subsynaptic polyribosomes. We report here a mechanism by which NMDAR activation at synapses may control this protein synthetic machinery. In intact tadpole tecta, NMDAR activation leads to phosphorylation of a subset of proteins, one of which we now identify as the eukaryotic translation elongation factor 2 (eEF2). Phosphorylation of eEF2 halts protein synthesis and may prepare cells to translate a new set of mRNAs. We show that NMDAR activation-induced eEF2 phosphorylation is widespread in tadpole tecta. In contrast, in adult tecta, where synaptic plasticity is reduced, this phosphorylation is restricted to short dendritic regions that process binocular information. Biochemical and anatomical evidence shows that this NMDAR activation-induced eEF2 phosphorylation is localized to subsynaptic sites. Moreover, eEF2 phosphorylation is induced by visual stimulation, and NMDAR blockade before stimulation eliminates this effect. Thus, NMDAR activation, which is known to mediate synaptic changes in the developing frog, could produce local postsynaptic alterations in protein synthesis by inducing eEF2 phosphorylation.**

Activation of *N*-methyl-D-aspartate receptors (NMDARs) has been implicated in many forms of synaptic plasticity. Much of this plasticity requires protein synthesis, presumably to express proteins needed to support altered synaptic function (1). Regulation of gene transcription is one way that NMDAR activation could be linked to altered protein expression (2). However, plasticity can be synapse specific, so neurons must have some way to target new proteins to the synapses producing the plasticity-inducing signal. The machinery for protein translation (3) and many mRNAs are localized within dendrites (4–6), but to date the precise mechanisms linking synaptic activation of NMDAR to local modulation of protein translation have not been fully characterized.

During development of many central nervous system pathways, NMDARs mediate synaptic competition and stabilization (7). This process has been extensively studied in the tadpole retinotectal projection because activity-dependent synaptic rearrangement is prolonged during tadpole life (8). Previous experiments in tadpole tecta described five proteins that become highly phosphorylated after NMDAR activation (9). We now show that one of these phosphoproteins is the eukaryotic translation elongation factor 2 (eEF2). This protein catalyzes ribosomal translocation along the mRNA. *In vitro*, eEF2 phosphorylation halts ribosomal translocation until eEF2 is dephosphorylated. Additionally, in the eukaryotic cells types studied to date, eEF2 phosphorylation is associated with reduced protein synthesis (10, 11). Phosphorylation of eEF2 is catalyzed by a single protein kinase, eEF2 kinase, whose activity is calcium- and calmodulin-dependent. Unlike many other calcium- and calmodulin-dependent kinases, eEF2 kinase phosphorylates a single substrate, eEF2 (12). Phosphorylation of eEF2 in other systems, such as during the cell cycle, precedes dramatic shifts in protein expression (11). Other links between protein synthesis inhibition and altered protein expression have been demonstrated (13). Finally, activation of amino acid neurotransmitter receptors is known to cause a reduction in protein synthesis (14, 15). Thus, eEF2 phosphorylation induced by synaptic activation of NMDARs could provide a mechanism for controlling protein composition at specific synapses.

MATERIALS AND METHODS

Front phosphorylation was carried out as previously described (9). Briefly, excised tecta were stimulated for 30 seconds in the presence of ^{32}P-labeled orthophosphate with a mixture of 10 μM glutamate and 50 μM NMDA. Tissue was homogenized and samples were separated by two-dimensional electrophoresis and transferred to nitrocellulose. Blots were exposed to x-ray film for 2–24 hr. After autoradiography, blots were probed with the phospho-specific anti-eEF2 antibody cc81 (1:200, ref. 15), and antibody–antigen binding was detected by using chemiluminescence. To verify that the two signals overlapped, exposures were used that generated both a chemiluminescence signal and an autoradiographic signal.

One-dimensional Western blotting was performed as previously described (16). Blots were probed with the phospho-specific antibodies as above. Densitometry was performed as previously described by using NIH IMAGE. Blots were then stripped and reprobed by using the affinity-purified pan-eEF2 antibody (G118, 1:500). Pan-eEF2 signals did not differ by more than 10% within blots, and these differences did not correlate with stimulation conditions.

The publication costs of this article were defrayed in part by page charge payment. This article must therefore be hereby marked "*advertisement*" in accordance with 18 U.S.C. §1734 solely to indicate this fact.

This paper was submitted directly (Track II) to the *Proceedings* office.
Abbreviations: NMDAR, *N*-methyl-D-aspartate receptor; NMDA, *N*-methyl-D-aspartate; GLUT, glutamate; eEF2, eukaryotic translation elongation factor 2; AP5, 2-amino-5-phosphopentanoic acid; TTX, tetrodotoxin; DAB, diaminobenzidine.
†To whom reprint requests should be addressed. e-mail: alfred.scheetz@yale.edu.

Electron microscopic localization was performed as previously described (17). Briefly, tecta were fixed, cryoprotected, quickly frozen, and stored at −70°C until use. Sixty- to 100-μm-thick vibratome sections were cut and processed for immunolocalization. Nonspecific binding was blocked with 5% normal serum and 1% nonfat dry milk. Horseradish peroxidase-linked secondary antibodies coupled with avidin-biotin amplification were used to detect antigen/antibody binding. Sections were then processed for conventional electron microscopy and viewed with a Zeiss EM-10 microscope.

For light-level immunocytochemistry, tecta were stimulated as above and fixed, cryoprotected, and frozen. Coronal or horizontal cryostat sections were cut at 10 μm. Slides containing at least one section from each of the stimulation conditions to be compared were processed for immunolocalization. Sections were permeabilized with 0.3% Triton X-100, and nonspecific binding was blocked with 10% BSA in PBS. Primary antibody dilutions used were 1:50 for cc81 and 1:500 for G118. Horseradish peroxidase-linked secondary antibodies were used to visualize eEF2 staining. Nucleus isthmus labeling was performed exactly as described (18).

Synaptoneurosomes, which are enriched in intact and functional pre- and postsynaptic structures, were prepared as previously described (19). Electron microscopy was performed to verify the composition of these suspensions. Synaptic density was comparable to values previously obtained (data not shown, but see Fig. 3*B*). Synaptoneurosome suspensions were diluted to a concentration of 1 mg/ml in bicarbonate buffer and allowed to equilibrate at 37°C for 30 min before drug stimulation. The samples were pelleted by centrifugation, homogenized in sample buffer, and prepared for immunoblot detection as above.

For *in vivo* visual stimulation, tadpoles were dark-adapted for 1 to 2 hr. All subsequent operations were performed in the dark with the aid of an infrared imaging system. Animals were briefly anesthetized with fresh 0.5% MS222 and a small hole made in the lateral sclera with an insect pin. A pipette filled with approximately 200 nl of 1 mM tetrodotoxin (TTX) was inserted into the hole, and the TTX was forced into the posterior chamber with pressure. The skull was then retracted to expose the tectum, and the dura was removed. The optokinetic reflex was used to activate a large population of retinal ganglion cells (20). Animals were placed into a hemispherical chamber containing 1-inch vertical bars spaced 2 inches apart. The chamber rotated at 0.25 Hz. Additionally, strobe lights, flashing at 0.5 Hz, were placed 10 inches away from the animal's eye. This stimulation lasted for 30 sec before 4% paraformaldehyde was immediately applied directly to the tectum. In some cases, a small dorsal area of retina in the active eye was shaded from the strobe light. The ventral region of tectum receiving input from this part of the retina thus provided an estimate of basal phospho-eEF2 levels in dark-adapted tecta.

Tissue was prepared as above for immunolocalization except that sections were coincubated with both anti-phospho-eEF2 (rabbit) and anti-tubulin (mouse). Immunolocalization was accomplished by visualizing the fluorescein-conjugated donkey anti-rabbit (phospho-eEF2) or Texas red-conjugated donkey anti-mouse (tubulin). Ten-micron sections were viewed with a Bio-Rad MRC 600 scanning confocal microscope. The two fluorophores were detected simultaneously, and the gain and offset were adjusted to give equivalent, nonsaturated pixel distributions. Single focal plane images were acquired and analyzed by using NIH IMAGE 1.60 and the Bio-Rad confocal macro written by Harvey Karten (University of California at

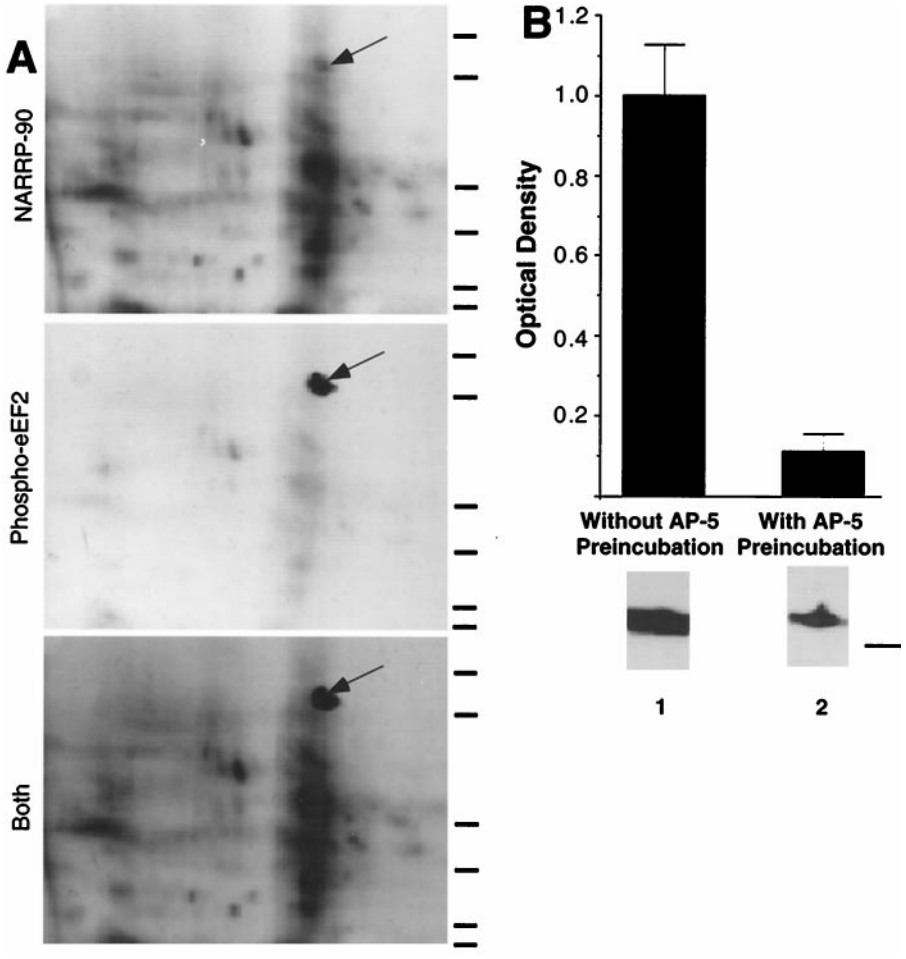

FIG. 1. NARPP-90 and eEF2 comigrate on blots of two-dimensional gels. (*A*) NARPP-90 phosphorylation was induced in tadpole tecta by NMDA/GLUT stimulation, the labeled proteins were blotted onto nitrocellulose, and NARPP-90 was detected by autoradiography (*Top*). The same blot was then probed with a phospho-specific anti-eEF2 antibody and the signal was detected with chemiluminescence (*Middle*). When a film was allowed to expose overnight after chemiluminescent detection, an image was produced that contained both radioactive and chemiluminescent signals (*Bottom*). This image shows that NARPP-90 and eEF2 have identical molecular masses and isoelectric points. Similar results were obtained in three other experiments. Molecular mass standards from bottom to top for each panel are 7.5, 18.2, 31.5, 42.7, 80, and 135 kDa. (*B*) Densitometric measurement of immunoblots detecting NMDAR-induced phospho-eEF2. Tecta received NMDA/GLUT stimulation with or without prior preincubation with 60 μM AP5. NMDA/GLUT stimulation alone resulted in a 7-fold increase in phospho-eEF2 compared with AP5 control (n = 5). NMDA/GLUT stimulation without AP5 preincubation produced robust eEF2 phosphorylation (lane 1). However, NMDA/GLUT stimulation after AP5 preincubation resulted in low levels of eEF2 phosphorylation (lane 2). To verify equal amounts of total eEF2 protein, all blots probed with the phospho-specific antibody were subsequently stripped and reprobed with the eEF2 antibody that does not distinguish between phospho- and dephospho-eEF2. The total amount of eEF2 did not vary as a function of stimulation (data not shown). The molecular mass standard for *B* is 80 kDa.

San Diego). Four line scans from the pia to ventricular surface per tectal lobe were taken for both tubulin and phospho-eEF2 images. To correct for inherent variability within the tissue processing and imaging procedure, the tubulin signal was used to normalize the phospho-eEF2 signal. Data from at least four sections per lobe from each animal were then averaged, and the ratio between the signal from the activated (left) tectum and the silenced (right) tectum was calculated. Data were pooled into 5-pixel bins and plotted as a function of distance from the pia.

RESULTS

Proteins phosphorylated by exposure of whole excised tadpole tectal lobes to a combination of 50 μM NMDA and 10 μM glutamate (GLUT) for 30 sec (hereafter called NMDA/GLUT stimulation) were previously termed NARPPs for *N*MDAR *a*ctivation *r*esponsive *p*hospho*p*roteins (9). One of these phosphoproteins, NARPP-90, has a molecular mass (90 kDa) and an isoelectric point (6.7–7.0) that are similar to those of eEF2 (10). NARPP-90 comigrates with phospho-eEF2 on two-dimensional gels, indicating that they are the same (Fig. 1*A*), and densitometric analysis of immunoblots by using a phospho-specific anti-eEF2 antibody (15) revealed a robust increase in phospho-eEF2 in NMDA/GLUT-stimulated excised tecta (Fig. 1*B*, lane 1). Preincubation with 60 μM AP5 for 5 min before NMDA/GLUT stimulation blocked the increase in phospho-eEF2 (Fig. 1*B*, lane 2). After the 30-sec NMDA/GLUT stimulation phospho-eEF2 levels declined to baseline by 10 min (data not shown, $n = 5$). Application of either component of NMDA/GLUT stimulation solution alone (10 μM glutamate or 50 μM NMDA) did not increase eEF2 phosphorylation over baseline (data not shown).

Synaptic remodeling within the retinotectal neuropil occurs locally among branches of retinal arbors and tectal dendrites (21). Light microscopic localization of phospho-eEF2 in NMDA/GLUT-stimulated tadpole tecta revealed label in dendrites throughout the retinorecipient layers (data not shown). To further examine this, tecta were processed for electron microscopic immunolocalization of phospho-eEF2. After NMDA/GLUT stimulation, strong phospho-eEF2 signal was localized to dendrites (Fig. 2*A*, asterisks). Often the

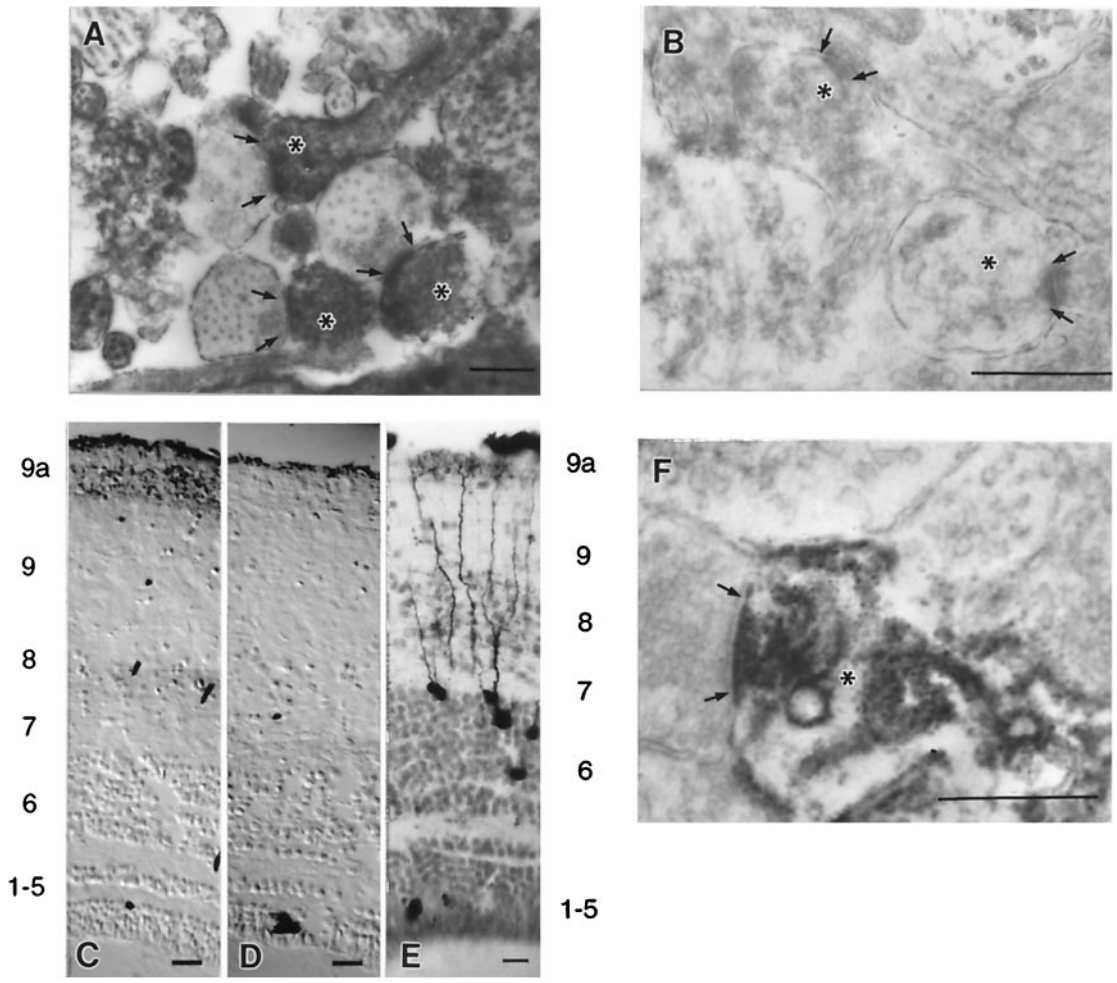

FIG. 2. Phospho-eEF2 in tecta detected by immunolocalization. Arrows delineate the presynaptic extent of the synaptic apposition, and asterisks mark dendritic profiles. (*A*) Electron micrograph of phospho-eEF2 immunostaining in the retinorecipient layers of tadpole tecta induced by NMDA/GLUT stimulation shows localization within dendrites. (*B*) Electron micrograph of phospho-eEF2 immunostaining induced by NMDA/GLUT stimulation after a 5-min preincubation with AP5 showed little or no phospho-eEF2. (*C*) Light-level micrograph of phospho-eEF2 immunostaining induced in adult frog tecta by NMDA/GLUT stimulation. (*D*) Light-level micrograph of phospho-eEF2 immunostaining in adult frog that received AP5 preincubation before NMDA/GLUT stimulation. No neuronal phospho-eEF2 staining was observed. (*E*) Tectal neurons that receive indirect ipsilateral retinal input via the nucleus isthmus have dense dendritic trees within layer 9a. Note that the layer labels for *C* and *D* correspond to the numbering on the left and the layers for *E* are on the right. (*F*) Electron micrograph of phospho-eEF2 immunostaining in adult frog tecta induced by NMDA/GLUT stimulation. This stimulation in adult tecta leads to preferential localization of phospho-eEF2 within dendritic segments subjacent to synaptic contacts in layer 9a. Pictures shown are representative of at least five independent determinations. Scale bars for *A*, *B*, and *F* represent 0.5 μm. Scale bars for *C–E* represent 50 μm.

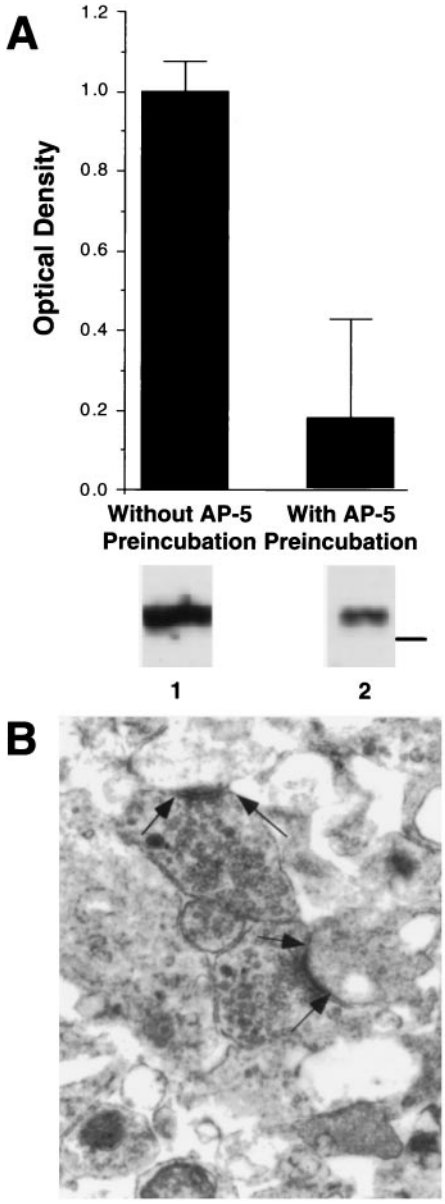

FIG. 3. Phospho-eEF2 is induced by NMDA/GLUT stimulation in preparations enriched in functional synaptic contacts. (*A*) Densitometric measurement of immunoblots detecting NMDAR-induced phospho-eEF2. Synaptoneurosomes received NMDA/GLUT stimulation with or without prior preincubation with 60 μM AP5. NMDA/GLUT stimulation alone resulted in a 7-fold increase in phospho-eEF2 compared with AP5 control. Examples shown are representative of three independent determinations. NMDA/GLUT stimulation without AP5 preincubation produced robust eEF2 phosphorylation (lane 1). However, NMDA/GLUT stimulation after AP5 preincubation resulted in low levels of eEF2 phosphorylation (lane 2). (*B*) Electron micrographs show that synaptoneurosomes are enriched in synaptic contacts. Arrows delineate presynaptic extent of synaptic apposition. Similar results were obtained from three independent synaptoneurosome preparations, and synaptic density is comparable to that reported previously (19).

electron-dense diaminobenzidine (DAB) reaction product produced dense floccular material that filled dendritic profiles and became associated with the postsynaptic densities (arrows mark the presynaptic side of the contact) in strongly labeled profiles. In contrast, phospho-eEF2 signal was absent from dendrites in tissue that had been preincubated with AP5 (Fig. 2*B*).

To determine whether eEF2 phosphorylation was correlated with the degree of synaptic plasticity within the retinotectal system, we compared phospho-eEF2 levels induced by NMDA/GLUT stimulation in tadpole and adult frog tecta. In adult frogs, synaptic remodeling is greatly reduced, and immunoblot analysis did not detect an increase in phospho-eEF2 levels with NMDA/GLUT stimulation compared with that obtained with AP5 preincubation (data not shown). However, by using DAB-based immunolocalization in adult tecta there was a small increase in phospho-eEF2 staining with NMDA/GLUT stimulation within a distinct, narrow band subjacent to the pial surface (Fig. 2 *C* without AP5, and *D* with AP5). This band corresponds to layer 9a and is present only in postmetamorphic frogs, where it is a site of binocular interaction. Tadpoles do not have a layer 9a because the pathway that carries the information from the opposite visual field does not reach the tectum until metamorphosis (18, 22). It is important to note that the dendritic segments located within this layer are far removed from their somata in layer 6 (Fig. 2*E*). Moreover, no neuronal cell bodies lie in layer 9a. Electron microscopic immunolocalization showed that, in adult tecta, NMDA/GLUT stimulation-induced phospho-eEF2 was absent from axons and was present only in dendrites within layer 9a, where the DAB reaction product produced dense floccular material that filled dendrites and often became associated with postsynaptic densities (Fig. 2*F*). These observations provide evidence that phospho-eEF2 levels are spatially regulated within tectal dendrites.

The results from the immunolocalization data suggest that eEF2 phosphorylation may occur at subsynaptic sites where dendritic ribosomes are often localized during synaptic development (23). To biochemically examine the subsynaptic localization of phospho-eEF2, synaptoneurosomes were prepared from tadpole tecta, and phospho-eEF2 levels were monitored. NMDA/GLUT stimulation increased phospho-eEF2 levels to an extent similar to that observed in whole excised tecta, and AP5 preincubation abolished this effect (Fig. 3*A*). Synaptoneurosome preparations are enriched in morphologically identifiable synaptic contacts containing both pre- and postsynaptic elements (Fig. 3*B*).

To examine whether visual stimuli could increase tectal phospho-eEF2 levels, one eye of dark-adapted tadpoles was treated with TTX to silence retinal ganglion cell activity. Both eyes then received unidirectional moving bar stimuli on a stroboscopic background for 30 sec. Tecta were immediately fixed and processed for phospho-eEF2 immunofluorescence localization. Anti-tubulin staining was used as an internal control for variations in staining. Bright immunofluorescence label for phospho-eEF2 was observed throughout the stimulated tecta (Fig. 4*A Upper*) and could be resolved within individual dendrites (Fig. 4*B*, arrows). In contrast, tectal lobes receiving input from the silenced eyes had considerably lower (darker) staining levels in their retinorecipient layers (Fig. 4*A Lower*). Scanning laser confocal microscopy was used to measure the immunofluorescence intensity for both phospho-eEF2 and tubulin across the same radial line scans on sections of each tectal lobe. Tubulin staining was uniform across the mediolateral and rostrocaudal extent of the tectum and did not vary as a function of stimulation condition (data not shown). By contrast, retinorecipient tectal layers receiving input from active eyes had two to three times more phospho-eEF2 immunofluorescence compared with layers receiving input from silenced eyes (Fig. 4*C*). This difference was decreased by application of AP5 to the exposed tectum for 5 min before the onset of visual stimulation. Fig. 4*D* shows the ratio between phospho-eEF2 signal in tecta receiving activated vs. silenced retinal input averaged across the retinorecipient layers.

DISCUSSION

Recent work has shown that far more transcripts are present in dendrites than had previously been suspected (4, 5, 24), as

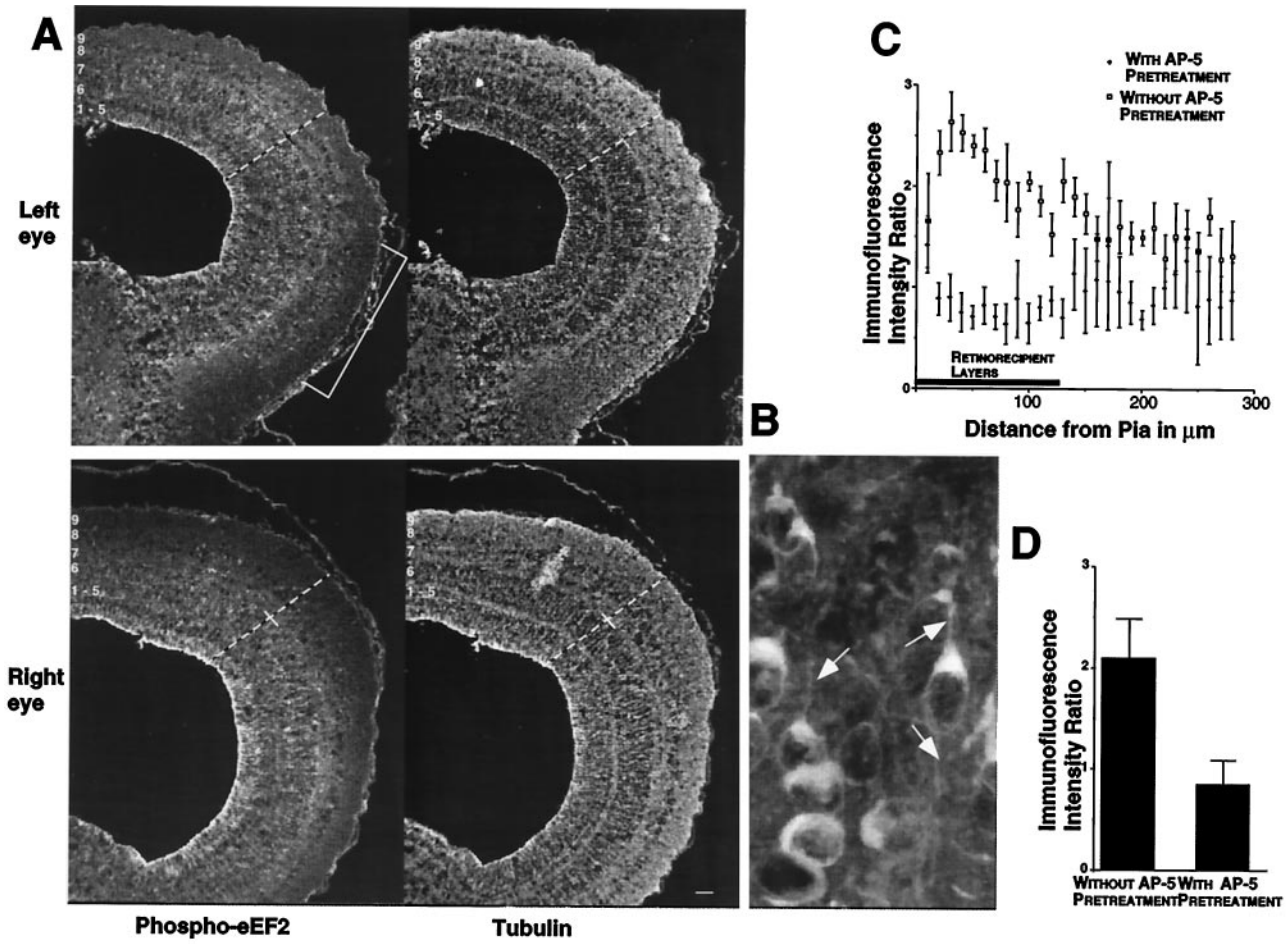

FIG. 4. Patterned visual stimulation causes eEF-2 phosphorylation within retinorecipient layers of the tadpole tectum. (*A*) Sections from tecta receiving either activated (*Upper*, left eye) or silenced (*Lower*, right eye) retinal input were stained for both phospho-eEF2 (*Left*, FITC) and tubulin (*Right*, Texas red). The white numbers indicate the location of the tectal layers. The dashed lines show representative line scans used for sampling fluorescence intensity. The small cross-hairs mark the boundary between the retinorecipient layers, 7–9, and the rest of the tectal layers. The white bracket shows the location of the ventral visual field projection that was shaded from the strobe and moving bar stimuli. This area of tectum provides an estimate of phospho-eEF2 levels caused by active but not directly stimulated retinal input. Signals for each fluorophore were imaged simultaneously from a single section. (*B*) A high magnification of tectal neurons and dendritic segments that are positive for eEF2 phosphorylation resulting from visual stimulation. Note the scattered punctate staining, which represents fine dendritic processes (arrows). (*C*) Laminar distribution of the ratio of phospho-eEF2 fluorescent signal in stimulated and silenced inputs in the absence (open squares) and presence (solid diamonds) of topically applied 60 μM AP5. The average location of retinorecipient layers is indicated by the bar along the abscissa. Error bars show the standard deviation of the average value from 5-pixel bins. (*D*) Histogram plots of the average ratio of phospho-eEF2 fluorescent signal between stimulated and silenced retinorecipient layers in the absence and presence of topically applied AP5. Error bars are the standard deviation derived from the average values for each individual used in the analysis ($n = 3$ with AP5 and $n = 5$ without AP5). Scale bar for *A* represents 50 μm.

are all the enzymes required for protein translation (4). Furthermore, dendrites are capable of responding to stimulation by increasing protein synthesis independent of cell body-based translational control (4, 25, 26). In hippocampal slices, dendritic protein synthesis is stimulated by correlated activation of cholinergic receptors and NMDARs (27). These observations suggest a functional link between local protein synthesis and synaptic activity (28). To date, *in situ* synaptic activation has not been linked to a mechanism that can modulate dendritic protein synthesis. We have shown that NMDAR activation elicited by sensory stimulation can cause phosphorylation of a protein critically involved in controlling protein synthesis at the peptide chain elongation step. This phosphorylation event may be particularly important for synaptic competition, as suggested by both the widespread distribution of phospho-eEF2 in tadpole dendrites, which support continuous activity-dependent synaptic rearrangement, and the specific localization of phospho-eEF2 at synaptic sites restricted to regions of tectal dendrites involved in processing binocular information in adult tecta.

Various forms of synaptic plasticity have been divided into early, protein synthesis-independent phases and late, protein synthesis-dependent phases (29–31). In many cases, the late phases seem to require both new translation and new transcription (1). Several models have been proposed to account for how the cell-wide nature of transcriptional control can lead to the synaptic specificity inherent in many forms of synaptic plasticity. These models postulate that proteins newly synthesized in the soma are targeted to the appropriate synapses via some form of synaptic tag produced at the time of the initial synaptic activation (32). Alternatively, synaptic activation could lead to the local synthesis of key proteins at the site of activation (33). The ability of eEF2 phosphorylation to alter synaptic protein translation could play important roles in either of these potential mechanisms.

Phosphorylation of eEF2 is correlated with a reduction of protein synthesis in many eukaryotic cells (11) including neurons (15). This is a somewhat paradoxical response to stimuli that should promote new protein synthesis; yet in many systems protein synthesis inhibition appears to be an early step

in the translation of a new set of transcripts (11). It is possible that transcripts that are being actively translated need to be removed from ribosomes before new transcripts can be initiated, and halting translation may promote this. Alternatively, inhibiting protein synthesis may permit less efficiently initiated transcripts to become translated (13). Finally, translational pausing could lead to reduced levels of short-lived repressor proteins that inhibit expression of other key proteins. Further studies are needed to examine these possibilities.

We have demonstrated that eEF2 phosphorylation is induced by visual stimulation in intact animals and depends on NMDAR activation. This suggests strongly that this event is a physiologically relevant response to synaptic NMDAR activation. The synaptic specificity of eEF2 phosphorylation is highlighted by the demonstration that it occurs within dendrites and at synaptic contacts. Furthermore, eEF2 phosphorylation can be spatially restricted to subsets of synaptic contacts within a given neuron. These properties qualify eEF2 phosphorylation as a potential component of a variety of mechanisms linking synaptic activity to protein synthesis-dependent synaptic plasticity. Phosphorylation of eEF2 represents a rapid, specific, and previously uncharacterized mechanism for inducing long-term changes in synaptic function.

We thank Tim Goldsmith for the use of the infrared dissection microscope, Haig Keshishian and the Neuroengineering and Neuroscience Center at Yale University for the use of the confocal microscope, and Sandra Aamodt and Rene Renteria for thoughtful discussions. The authors also thank Gloria Bertuzzi for technical assistance in preparation of the antibodies and Jane Sibley for help with the electron microscopy. This work was supported by U.S. Public Health Service Grant EY 06039 to M.C.P. and GM 50402 to A.C.N.

1. Schuman, E. (1997) *Neuron* **18,** 339–342.
2. Bading, H., Segal, M. M., Sucher, N. J., Dudek, H., Lipton, S. A. & Greenberg, M. E. (1995) *Neuroscience* **64,** 653–664.
3. Tiege, H. & Brosius, J. (1996) *J. Neurosci.* **16,** 7171–7181.
4. Crino, P. B. & Eberwine, J. (1996) *Neuron* **17,** 1173–1187.
5. Miyashiro, K., Dichter, M. & Eberwine, J. (1994) *Proc. Natl. Acad. Sci. USA* **91,** 10800–10804.
6. Steward, O. (1995) *Curr. Opin. Neurobiol.* **5,** 55–61.
7. Scheetz, A. J. & Constantine-Paton, M. (1994) *FASEB J.* **8,** 7445–7452.
8. Reh, T. A. & Contantine-Paton, M. (1984) *J. Neurosci.* **4,** 442–457.
9. Scheetz, A. J. & Constantine-Paton, M. (1996) *J. Neurosci.* **15,** 1460–1469.
10. Nairn, A. C. & Palfrey, H. C. (1996) in *Translational Control*, eds. Hershey, J. W. B., Mathews, M. B. & Sonenberg, N. (Cold Spring Harbor Lab. Press, Plainview, NY), pp. 295–318.
11. Ryazanov, A. G. & Spirin, A. S. (1993) in *Translational Regulation of Gene Expression*, ed. Iian, J. (Plenum, New York), pp. 433–455.
12. Mitsui, K., Brady, M., Palfrey, H. C. & Nairn, A. C. (1993) *J. Biol. Chem.* **268,** 13422–13433.
13. Walden, W. E., Godefory-Colburn, T. & Thach, R. E. (1981) *J. Biol. Chem.* **256,** 11739–11746.
14. Orrego, F. & Lipman, F. (1967) *J. Biol. Chem.* **242,** 665–671.
15. Marin, P., Nastuik, K. L., Girault, J.-A., Czernik, A. J., Glowinski, J., Nairn, A. C. & Prémont, J. (1997) *J. Neurosci.* **17,** 3445–3454.
16. Scheetz, A. J., Prusky, G. T. & Constantine-Paton, M. (1996) *Eur. J. Neurosci.* **8,** 1322–1328.
17. Scheetz, A. J. & Dubin, M. W. (1994) *Brain Res.* **639,** 181–192.
18. Law, M. I. & Constantine-Paton, M. (1982) *Brain Res.* **247,** 201–208.
19. Hollingsworth, E. B., McNeal, E. T., Burton, J. L., Williams, R. J., Daly, J. W. & Creveling, C. R. (1985) *J. Neurosci.* **5,** 2240–2253.
20. Ingle, D. (1976) in *Frog Neurobiology*, eds. Llinás, R. & Precht, W. (Springer, New York), pp. 435–451.
21. Yen, L.-H., Sibley, J. & Constantine-Paton, M. (1992) *J. Neurosci.* **13,** 4949–4960.
22. Udin, S. B., Fisher, M. D. & Norden, J. J. (1980) *J. Comp. Neurol.* **292,** 246–254.
23. Steward, O. & Falk, P. M. (1991) *J. Comp. Neurol.* **314,** 545–557.
24. Link, W., Konietzko, U., Kauselmann, G., Krug, M., Schanke, B., Frey, U. & Kuhl, D. (1995) *Proc. Natl. Acad. Sci. USA* **92,** 5734–5738.
25. Weiler, I. J., Irwin, S. A., Klintsova, A. Y., Spencer, C. M., Brazelton, A. D., Miyashiro, K., Comery, T. A., Patel, B., Eberwine, J. & Greenough, W. T. (1997) *Proc. Natl. Acad. Sci. USA* **94,** 5395–5400.
26. Weiler, I. J. & Greenough, W. T. (1993) *Proc. Natl. Acad. Sci. USA* **90,** 7168–7171.
27. Feig, S. & Lipton, P. (1993) *J. Neurosci.* **13,** 1010–1021.
28. Steward, O. (1997) *Neuron* **18,** 9–12.
29. Frey, U., Krug, M., Brodemann, R., Reymann, K. & Matthies, H. (1989) *Neurosci. Lett.* **97,** 135–139.
30. Goelet, P., Castellucci, V. F., Schacher, S. & Kandel, E. R. (1986) *Nature (London)* **322,** 419–422.
31. Linden, D. J. (1996) *Neuron* **17,** 483–490.
32. Frey, U. & Morris, R. G. (1997) *Nature (London)* **385,** 533–536.
33. Kang, H. & Schuman, E. M. (1996) *Science* **273,** 1402–1406.